

Simultaneous X-ray and VHE γ -ray observations of microquasars

P.M. Chadwick, H.J. Dickinson, I.J. Latham, S.J. Nolan, J.L. Osborne
for the H.E.S.S. collaboration.

University of Durham, South Road, Durham, United Kingdom.

Presenter: S.J. Nolan (s.j.nolan@dur.ac.uk), uki-nolan-S-abs1-og22-poster

In a search for episodic TeV emission, H.E.S.S. observations of the microquasar objects V4641 Sgr, GRS1915+105, Cir-X1 and GX339-4 are reported. Some observations were made simultaneously with the RXTE satellite, and in such cases we also present the results of the analysis of the RXTE data.

1. Introduction

Despite being relatively few in number, the current catalogue of known galactic microquasars represents an exciting laboratory with which to probe the non-thermal Universe. With a nomenclature derived from their structural similarities with Active Galactic Nuclei (AGNs), microquasars offer an enticing opportunity to disentangle the processes of accretion and ejection around compact objects. Indeed, if morphology is significantly linked to underlying physical processes, then microquasars may exhibit the TeV γ -ray emission already observed in their supermassive cousins.

Although the physical components of AGNs and microquasars (i.e. a central black hole, an accretion disc and collimated jets of relativistic particles) show remarkable similarities, the two object classes differ radically on scales of size, luminosity, variability time and distance. At $\sim 10M_{\odot}$, the central black hole masses of galactic microquasars pales when compared to the $\sim 10^9M_{\odot}$ central engines observed in AGNs. A major consequence of this disparity in mass is the plausible opportunity to probe for gamma-ray emission and its possible correlation with X-ray emission in different astrophysical environments.

The much lower power of the microquasars compared to that of the AGN is offset by their closeness to Earth. As an indication of likely microquasar fluxes, the parameter L_{Edd}/d^2 , where L_{Edd} is the Eddington luminosity and d is the distance from Earth, is typically 2-4 orders of magnitude higher for microquasars than AGNs [1].

Contemporaneous X-ray and VHE γ -ray spectra of AGN have been instrumental to the study of associated processes at the highest energies. By extension, it is hoped that similar multiwavelength studies of microquasars will offer new revelations in our understanding of jet formation and the complex environments around compact accretors.

In this paper we present observations of four galactic microquasars, using the *Rossi X-ray Timing Explorer* (RXTE) in combination the *High Energy Stereoscopic System* (H.E.S.S.) Imaging Atmospheric Cherenkov Telescope (IACT) array in the Khomas Highlands, Namibia. The goal of the study was to obtain simultaneous VHE γ -ray and X-ray spectra from each target during an energetic outburst event. Consequently, the chosen targets (shown in table 1) were selected primarily on the basis of their well studied variability behaviour and previously observed outbursts.

2. Observations

Table 1 lists the H.E.S.S. and RXTE observation epochs for each of the four target microquasars. X-ray observations of GRS1915+105 were hoped to coincide with predicted superluminal ejections from the source [2]. In the case of V4641 Sgr, the detection of a series of small outbursts reminiscent of those observed prior to

Table 1. Observational Targets and Epochs

Target	RXTE Observations (MJD)	H.E.S.S. Observations (MJD)	Overlap Time (MJD)
GRS1915+105	53123.090 → 53123.109 53127.096 → 53127.114 53128.149 → 53128.164	53123.066 → 53123.149 53127.106 → 53127.164 53128.148 → 53128.164	53123.090 → 53123.109 53127.106 → 53127.114 53128.149 → 53128.164
V4641 Sgr	53193.903 → 53193.923 53194.885 → 53194.907 53195.870 → 53195.892	Not Observed 53194.883 → 53194.909 53195.889 → 53195.906	N/A 53194.885 → 53194.907 53195.889 → 53195.892
GX339-4	Not Observed	53229.772 → 53229.869 53230.756 → 53230.913 53231.807 → 53231.904	N/A N/A N/A
Circinus X-1	53174.746 → 53174.760 53175.767 → 53175.780 53176.781 → 53176.793	53174.747 → 53174.831 53175.734 → 53175.821 53176.771 → 53176.857	53174.747 → 53174.760 53175.767 → 53175.780 53176.781 → 53176.793

the 1999 12 crab X-ray outburst [3] precipitated the *RXTE* trigger. Observations of Circinus X-1 were timed to coincide with the periastron zero phase of the system, and GX-339-4 remained unobserved in X-rays in deference to a competing *H.E.S.S.* multiwavelength campaign involving the BL Lac object PKS 2155-304.

X-ray data were obtained using two *RXTE* instruments: the *Proportional Counter Array (PCA)*, and the *High Energy X-ray Timing Explorer (HEXTE)* clusters. The full 4-IACT configuration of *H.E.S.S.* array was used for the simultaneous VHE γ -ray observations.

3. Results

The measured X-ray spectra of GRS1915+105, V4641 Sgr and Circinus X-1 are shown in figures 1, 2 and 3, respectively. Also shown are the physically motivated models fitted to the data using XSPEC [4]. The chosen model, WABS*(DISKBB+POWERLAW+GAUSS) is consistent with thermal emission from an accretion disk with Fe $K\alpha$ fluorescent line emission. Table 2 contains estimated model 3.0-10keV fluxes and [6.5-10keV]/[3.0-6.5keV] hardness ratios for each of the sources observed in the X-ray band.

Table 2. Model X-ray Fluxes and *H.E.S.S.* Integral Flux Upper Limits above a threshold of 1 TeV for ease of comparison. Also shown is the average energy threshold of the observations for each source.

Target	Integral X-ray Flux [3.0-10.0keV] [$\text{cm}^{-2}\text{s}^{-1}$]	X-Ray Hardness Ratio [6.5-10keV]/[3.0-6.5keV]	<i>H.E.S.S.</i> Upper Limit [>1TeV] [$\text{cm}^{-2}\text{s}^{-1}$]	<i>H.E.S.S.</i> $\langle E_t \rangle$ [TeV]
GRS1915+105	0.5195	0.28	3.69×10^{-13}	0.50
V4641 Sgr	1.91×10^{-3}	0.41	9.21×10^{-13}	0.165
GX339-4	N/A	N/A	6.92×10^{-13}	0.25
Circinus X-1	1.796×10^{-2}	0.19	9.22×10^{-13}	0.50

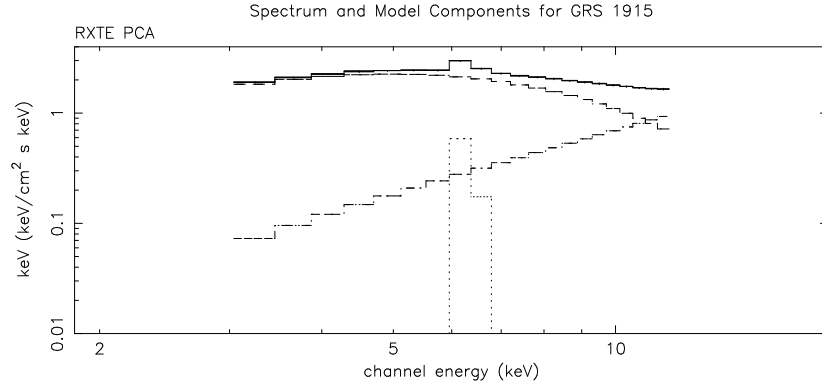


Figure 1. RXTE PCA Spectrum and XSPEC Model for GRS1915+105. Component parts of the fitted model are shown as lines, data as points. χ^2 per degree of freedom for this fit was 3.29, which may suggest the unusual behaviour of GRS1915+105.

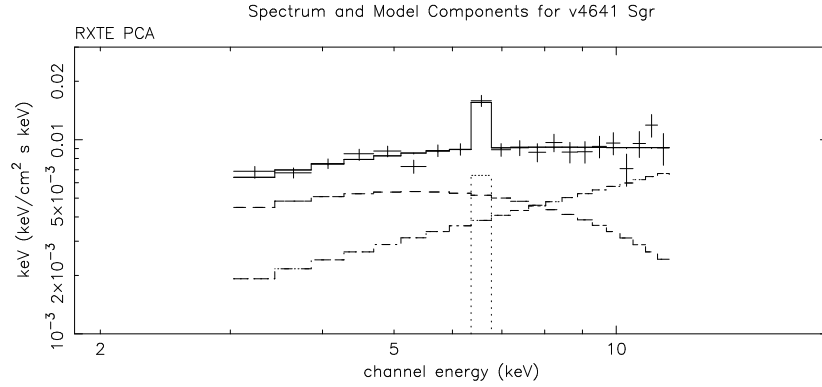


Figure 2. RXTE PCA Spectrum and XSPEC Model for V4641 Sgr. Component parts of the fitted model are shown as lines, data as points. χ^2 per degree of freedom for this fit was 1.2.

Table 2 also lists the *H.E.S.S.* 90% confidence upper limits for all four microquasars, none of the targets being detected with *H.E.S.S.*. This value is obtained using confidence intervals generated via the Feldman-Cousins approach and relies on an assumed differential photon index for the source. For our microquasars, this index was assumed to be $\alpha = -2.0$. It should be noted that there are no current models which could associate gamma-ray emission with the accretion disk. However, the upper limit is relatively insensitive to changes in spectral slope.

4. Discussion

The lack of a conclusive *H.E.S.S.* detection, and consequently the absence of any VHE γ -ray spectra or lightcurves denies insight into many of the phenomena discussed in §1. Nonetheless, the upper limits obtained do place useful constraints on the TeV emission of microquasars in given X-ray states.

It is apparent on inspection of the X-ray data that despite indications to the contrary, none of the targets were

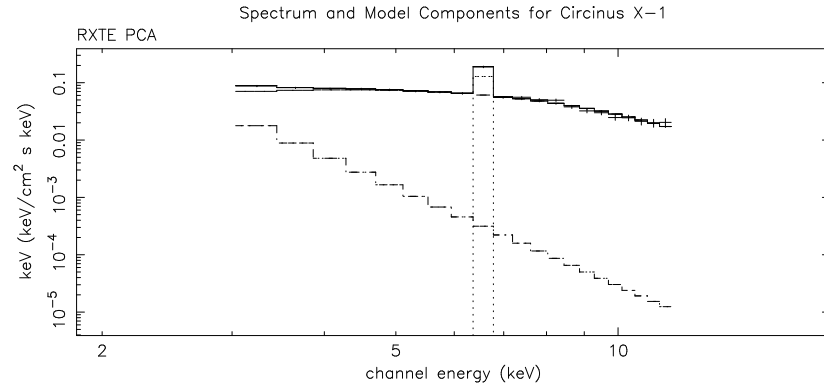


Figure 3. RXTE PCA Spectrum and XSPEC Model for Circinus X-1. Component parts of the fitted model are shown as lines, data as points. χ^2 per degree of freedom for this fit was 1.38.

behaving in an abnormally energetic manner at the time of observation. Indeed, the *PCA* spectra obtained are consistent with those of X-ray binaries in the high-soft state (e.g. [6]), while *HEXTE* observations, excepting GRS1915+105, are consistent with zero flux.

In our current understanding of microquasar systems, the most significant gamma-ray emission is likely to be just before a superluminal radio ejection, which in itself is linked to dramatic X-ray stage changes [7]. Unfortunately as can be seen this dataset does not contain such behaviour. The LS5039 system has a massive luminous companion, and in contrast to these objects a much steadier jet, which may have aided its recent detection by HESS [8].

5. Conclusions

Although no detections are discussed within this paper, the unprecedented sensitivity of *H.E.S.S.* in the TeV regime, makes it the ideal instrument for further studies of microquasar objects. With the discovery of gamma-ray emission from LS 5039 by *H.E.S.S.* [8], it is surely only a matter of time before VHE emission is seen from other microquasars.

References

- [1] Atoyan, A., & Aharonian, F.A., High Energy Gamma Ray Astronomy Symp., AIP Conf. Proc. vol. 558, 234 (2001)
- [2] Pooley, G., Private Communication (2004)
- [3] Hjellming, R. M., Rupen, M. P., Hunstead, R. W., Campbell-Wilson, D., Mioduszewski, A. J., Gaensler, B. M., Smith, D. A., Sault, R. J., Fender, R. P., Spencer, R. E., de la Force, C. J., Richards, A. M. S., Garrington, S. T., Trushkin, S. A., Ghigo, F. D., Waltman, E. B., McCollough, M., ApJ. 544, 977 (2000)
- [4] Arnaud K.A., in Jacoby G.H., Barnes J., eds, ASP Conf. Series 101, 17 (1996)
- [5] Kardashev, N.S., Soviet Astr.-A.J. 6, 317 (1962)
- [6] Done, C., Advances in Space Research 28, 255 (2000)
- [7] Fender, R., et al., MNRAS, 288, 849 (1997)
- [8] de Naurois, M., & Dubus, G., in these proceedings, (2005)